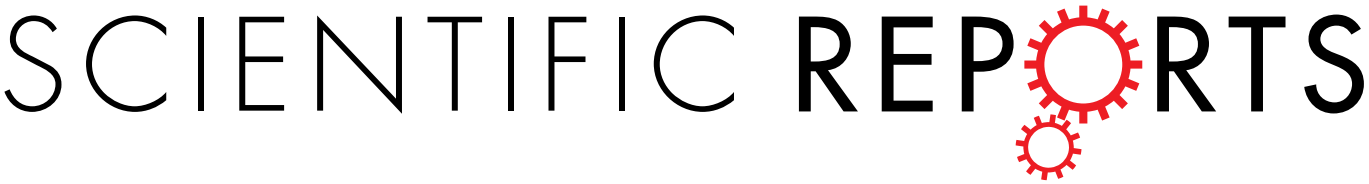

OPEN

Probing the Structural and Electronic Properties of Dirhenium Halide Clusters: A Density Functional Theory Study

Received: 15 February 2018
Accepted: 13 April 2018
Published online: 30 April 2018

Li Huan Zhang[1,2], Xin Xin Xia[1], Wei Guo Sun[1], Cheng Lu[2,3], Xiao Yu Kuang[1], Bo Le Chen[1] & George Maroulis[4]

Dirhenium halide dianions received considerable attention in past decades due to the unusual metal–metal quadruple bond. The systematic structural evolution of dirhenium halide clusters has not been sufficiently studied and hence is not well-understood. In this work, we report an in-depth investigation on the structures and electronic properties of doubly charged dirhenium halide clusters $Re_2X_8^{2-}$ (X = F, Cl, Br, I). Our computational efforts rely on the well-tested unbiased CALYPSO (Crystal structure AnaLYsis by Particle Swarm Optimization) method combined with density functional theory calculations. We find that all ground-state $Re_2X_8^{2-}$ clusters have cube-like structures of D_{4h} symmetry with two Re atoms encapsulated in halogen framework. The reasonable agreement between the simulated and experimental photoelectron spectrum of the $Re_2Cl_8^{2-}$ cluster supports strongly the reliability of our computational strategy. The chemical bonding analysis reveals that the δ bond is the pivotal factor for the ground-state $Re_2X_8^{2-}$ (X = F, Cl, Br, I) clusters to maintain D_{4h} symmetric cube-like structures, and the enhanced stability of $Re_2Cl_8^{2-}$ is mainly attributed to the chemical bonding of 5d orbital of Re atoms and 3p orbital of Cl atoms.

The discovery[1] of the metal–metal quadruple bond in dirhenium halide $Re_2Cl_8^{2-}$, which is recognized as an important milestone in the development of modern inorganic chemistry, has stimulated intensive research work in the field of transition metal chemistry[2,3]. Understanding the properties of the metal–metal multiple bond is significant to further elucidate the chemistry of transition metal complexes. As a prototypical metal–metal multiple bonded ion, $Re_2Cl_8^{2-}$ has been studied extensively in the past decades[2,4–22]. The experimental and theoretical investigations mainly focused on the preparation[4–6], the molecular structure[7,8], the metal–metal multiple bond[2,9–14] and the electronic properties[4,10,15–22] of $Re_2Cl_8^{2-}$ in the octachlorodirhenate salts. Previous studies[7–13] have determined the geometry structure of $Re_2Cl_8^{2-}$ to be of D_{4h} symmetry, and confirmed the formation of Re–Re quadruple bond is due to the $\sigma^2\pi^4\delta^2$ subset of the bonding orbitals. Due to the difficulty of preparing the $Re_2Cl_8^{2-}$ dianion in the gas phase, Wang *et al.*[21] first measured the photoelectron spectrum (PES) of gaseous $Re_2Cl_8^{2-}$ several decades after the discovery of the metal−metal multiple bond, leading to a thorough understanding of the Re–Re quadruple bond and its electronic structure.

Compared to the extent of the investigations on $Re_2Cl_8^{2-}$, similar treatments of the heavier halogen derivative $Re_2Br_8^{2-}$, which contains the Re–Re quadruple bond as well, are limited[4,17,23,24]. To our knowledge, sparse studies have been reported on the lighter halogen derivative $Re_2F_8^{2-}$. Peters *et al.*[25] initially synthesized $(n\text{-}Bu_4N)_2[Re_2F_8]\cdot 4H_2O$, which contains $Re_2F_8^{2-}$, via $Re_2Cl_8^{2-}$ and $(n\text{-}Bu_4N)F\cdot 3H_2O$ reacting in CH_2Cl_2 solution. Conradson *et al.*[26] later confirmed the presence of the Re–Re quadruple bond in $Re_2F_8^{2-}$ using X-ray absorption fine structure and resonance Raman spectroscopy. The structure of $Re_2F_8^{2-}$ was determined to be eclipsed D_{4h} geometry by Henkel *et al.*[27]. Recently, Balasekaran *et al.*[28] prepared the $(NH_4)_2[Re_2F_8]\cdot 2H_2O$ salt in nearly 90% yield by the reaction of $(n\text{-}Bu_4N)_2[Re_2Cl_8]$ with molten NH_4HF_2. They also investigated the molecular and electronic structure along with

[1]Institute of Atomic and Molecular Physics, Sichuan University, Chengdu, 610065, China. [2]Department of Physics, Nanyang Normal University, Nanyang, 473061, China. [3]Department of Physics and High Pressure Science and Engineering Center, University of Nevada, Las Vegas, Nevada, 89154, United States. [4]Department of Chemistry, University of Patras, GR-26500, Patras, Greece. Correspondence and requests for materials should be addressed to C.L. (email: lucheng@calypso.cn) or X.Y.K. (email: scu_kuang@163.com) or G.M. (email: maroulis@upatras.gr)

the electronic absorption spectrum of $Re_2F_8^{2-}$ relying on multiconfigurational quantum chemical calculations. Compared to $Re_2F_8^{2-}$, studies on $Re_2I_8^{2-}$ are sparse as well. Glicksman *et al.*[29] firstly reported a synthesis route of $Re_2I_8^{2-}$ via the reaction of the dirhenium complex $Re_2(O_2CC_6H_5)_4Cl_2$ and HI with Bu_4N^+ in ethanol or methanol to produce the $(Bu_4N)_2Re_2I_8$ salt. Preetz *et al.*[30] prepared $(Bu_4N)_2Re_2I_8$ successfully for the first time in a simple procedure by the reaction of $(Bu_4N)_2Re_2X_8$ with HI in dichloromethane. Preetz *et al.*[31] also reported measurements of the resonance Raman spectrum of $(Bu_4N)_2Re_2I_8$, while Cotton *et al.*[32] studied its crystal structure until a few years later. Extensive studies on $Re_2X_8^{2-}$ have been reported, but almost all previous studies focused on $Re_2X_8^{2-}$ dianions in crystals. There has been no systematic work on $Re_2X_8^{2-}$ (X = F, Cl, Br and I) clusters until now, so the following questions attract our interests: (i) It is not clear whether $Re_2X_8^{2-}$ clusters are characterized by the same molecular geometry as $Re_2X_8^{2-}$ dianions in crystals. (ii) Does the chemical bonding in $Re_2X_8^{2-}$ clusters differ from that of dianions in crystals? (iii) What is the relative stability of $Re_2X_8^{2-}$ clusters? Consequently, we turn our attention to the systematic study of lowest-energy geometries and electronic structures of $Re_2X_8^{2-}$ (X = F, Cl, Br, I) clusters.

As a first step of our study on the structural evolution of $Re_2X_8^{2-}$ clusters, we perform a search for the the low-energy structures of $Re_2X_8^{2-}$ (X = F, Cl, Br, I) by means of the CALYPSO (Crystal structure AnaLYsis by Particle Swarm Optimization) code combined with DFT (density functional theory) calculations. We get the ground-state structures of $Re_2X_8^{2-}$ clusters from the above calculations and subsequently investigate their relative stabilities and chemical bonding. This paper is organized as follows. The obtained results and a pertinent discussion are in the following. Then we summarize our conclusions. Last, a detailed presentation of the computational method is described.

Results and Discussion

Geometric Structure. The lowest-energy structures of the $Re_2X_8^{2-}$ (X = F, Cl, Br, I) clusters, together with other three typical low-lying isomers are shown in Fig. 1. The optimized vibrational frequencies and atomic coordinates of ground-state $Re_2X_8^{2-}$ (X = F, Cl, Br, I) clusters are all collected in Table S1 and Table S2 of the supplementary information. According to their energies from low to high, all isomers are denoted by na, nb, nc and nd (n = 1, 2, 3,4), in which a, b, c and d stand for $Re_2F_8^{2-}$, $Re_2Cl_8^{2-}$, $Re_2Br_8^{2-}$ and $Re_2I_8^{2-}$, respectively. The electronic states, point group symmetries, average binding energies, HOMO−LUMO (the highest occupied molecular orbitals and the lowest unoccupied molecular orbitals) energy gaps, together with charge on Re atoms and halogen atoms of the ground-state $Re_2X_8^{2-}$ clusters are summarized in Table 1. In addition, the electronic states, point group symmetries, relative energies, HOMO−LUMO energy gaps of all isomers are given in Table S3.

It can be seen in Fig. 1 that the ground state 1a, 1b, 1c and 1d of $Re_2X_8^{2-}$ (X = F, Cl, Br, I) all possess cube-like geometric structures with D_{4h} symmetry. The geometric structures of ground-state $Re_2X_8^{2-}$ (X = F, Cl, Br, I) clusters favor low-spin $^1A_{1g}$ state and have the same symmetry with those in crystals[2,7,11,23,27,32]. With the increase of the halogen atom size, the Re–Re bond length in $Re_2X_8^{2-}$ varies from $Re_2F_8^{2-}$ to $Re_2I_8^{2-}$ as 2.20 Å, 2.21 Å, 2.22 Å, 2.24 Å, showing a little difference to those of $Re_2X_8^{2-}$ dianions in crystal[2]. The 2a isomer has a distorted cube-like structure with C_2 symmetry and the energy is 1.14 eV higher than its ground-state structure 1a. The metastable isomer 3a of $Re_2F_8^{2-}$ has C_s symmetry, at 1.71 eV higher than its global minimum 1a. Interestingly enough, the structure of 3a is a small square-bottom boat, and the two rhenium atoms are located in its interior. The point group symmetry of the 4a isomer is C_{2v}, and its energy is 3.36 eV higher than its lowest-energy structure 1a. It is obvious that the two rhenium atoms are exposed outside in the geometry structure of 4a. It can be clearly seen from Fig. 1 that 2b has similar structures with 3a. The isomer of 2b has C_1 symmetry with its energy 1.16 eV higher than the ground-state structure 1b. The isomers of 3b and 4b display cage-like structure with the two Re atoms encapsulated in a chlorine framework. They possess C_s and C_{2v} symmetry with the energy 1.22 eV and 1.47 eV, respectively, higher than their lowest-energy structures 1b. The isomer 2c has C_{2v} symmetry, with total energy 0.28 eV higher than the ground-state 1c, whose structure is similar to that of 2b. The 3c structure of C_{2v} symmetry looks similar to the structure of 4b, with total energy higher than 1c by 1.31 eV. The C_{2v} symmetry 4c isomer is 3.07 eV less stable than the ground-state 1c. The 2d isomer of C_{2v} symmetry has similar structure to the isomers 2b and 2c with the total energy 0.43 eV higher than 1d structure. The structure of 3d, which possesses D_{2d} symmetry with total energy higher than the 1d one by 1.50 eV, is similar to that of 4b and 3c isomers. The C_{2v} symmetry 4d isomer, at 2.43 eV higher in energy than the ground-state 1d, has similar structure to 4c. It is worth noting that, except for the 4a structure of $Re_2F_8^{2-}$, the two rhenium atoms are invariably inclined to stay inside for all ground and excited state structures of $Re_2X_8^{2-}$ (X = F, Cl, Br, I). In order to confirm the validity of our calculations, we have also optimized the $Re_2X_8^{2-}$ (X = F, Cl, Br, I) clusters at the BP86 level of theory. The corresponding lowest-energy geometries of $Re_2X_8^{2-}$ clusters are presented in Figure S1 of the supplementary information. From Figure S1 we can see all structures optimized at BP86 functional also have cube-like structures with D_{4h} symmetry and the same electronic state of $^1A_{1g}$. The respective ground-state structures are in agreement with those obtained by our B3LYP optimization, further supporting our claim for the reliability of our theoretical approach.

Photoelectron Spectra of $Re_2X_8^{2-}$. Photoelectron spectrum (PES) is a powerful tool, which can provide important information about the electronic configuration of ground-state structures. In order to verify the validity of our obtained structures in this work, as shown in Fig. 2, we have simulated the photoelectron spectra of all global minimum geometries of $Re_2X_8^{2-}$ (X = F, Cl, Br, I) and compared to the available experimental PES. Moreover, the values of adiabatic detachment energy (ADE), extracted from the threshold of the first peak, and the values of vertical detachment energy (VDE), obtained from the first peak maximum of the spectra, are summarized in Table S5 together with the available experimental data[21].

As shown in Fig. 2, all spectra exhibit rich features, which correspond to transitions from the ground state of $Re_2X_8^{2-}$ to the ground and excited states of singly charged $Re_2X_8^-$. Overall, the binding energies, spacings and intensities are different in each spectrum, but the spacings and intensities of spectra features for $Re_2Br_8^{2-}$ and

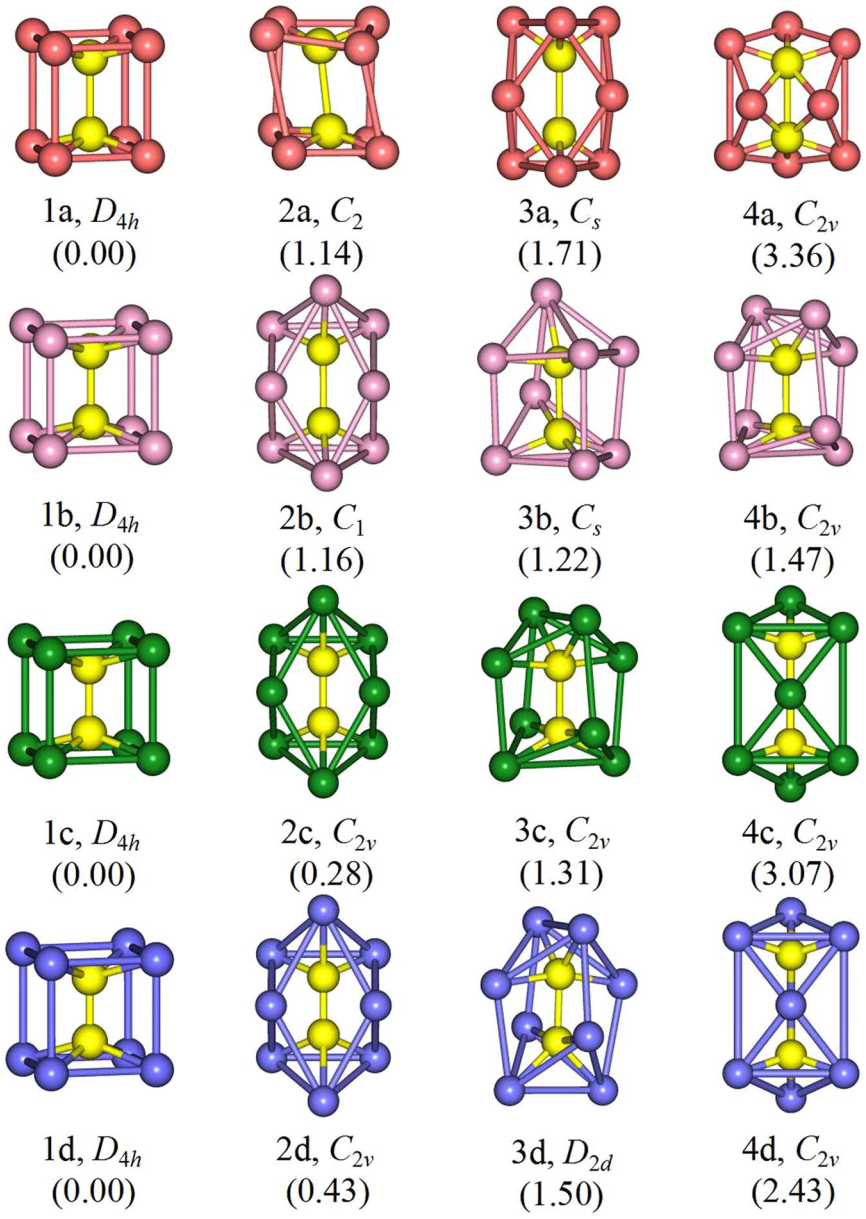

Figure 1. The geometrical structures of low-lying $Re_2X_8^{2-}$ (X = F, Cl, Br, I) clusters, along with the point group symmetry and relative energy (eV). Rhenium atoms are in yellow. Fluorine, chlorine, bromine and iodine atoms are in orange, pink, green and purple, respectively.

Cluster	State	Sym.	E_b	E_{gap}	Q (Re)	Q (X)
$Re_2F_8^{2-}$	$^1A_{1g}$	D_{4h}	3.91	1.94	1.29	−0.57
$Re_2Cl_8^{2-}$	$^1A_{1g}$	D_{4h}	2.49	1.71	−0.03	−0.24
$Re_2Br_8^{2-}$	$^1A_{1g}$	D_{4h}	2.07	1.66	−0.32	−0.17
$Re_2I_8^{2-}$	$^1A_{1g}$	D_{4h}	1.72	1.43	−0.60	−0.10

Table 1. Electronic states, point group symmetries, average binding energies E_b (eV), HOMO−LUMO energy gaps E_{gap} (eV) along with charge Q (e) on Re atoms and halogen atoms of $Re_2X_8^{2-}$ (X = F, Cl, Br, I) clusters.

$Re_2I_8^{2-}$ are nearly similar to each other. The most prominent spectral feature of $Re_2F_8^{2-}$ is the observation of a lower adiabatic detachment energy measured as 0.05 eV. This phenomenon is normal for multiply charged anions, largely due to the presence of intramolecular Coulomb repulsion[33,34]. It can be clearly seen that the first two peaks of the $Re_2F_8^{2-}$ spectrum are very weak and appear in very lower binding energies. The following relatively intense peaks locate at 1.25 and 1.70 eV, respectively, and the most intense peak locates at 3.80 eV. For the

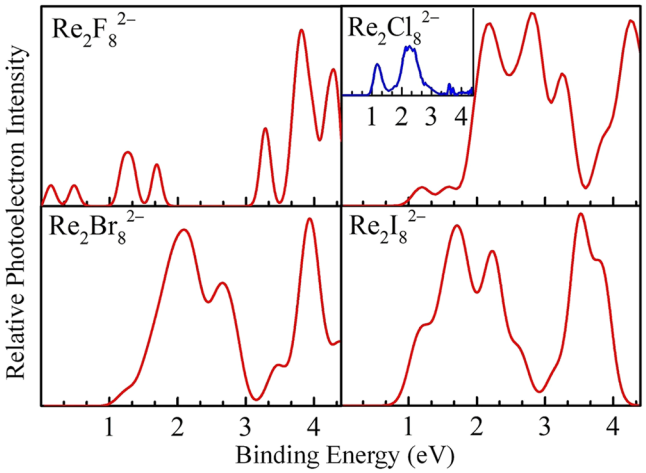

Figure 2. The simulated photoelectron spectra of the ground-state structures of $Re_2X_8^{2-}$ (X = F, Cl, Br, I) clusters, along with the available experimental spectrum of $Re_2Cl_8^{2-}$ in the inset.

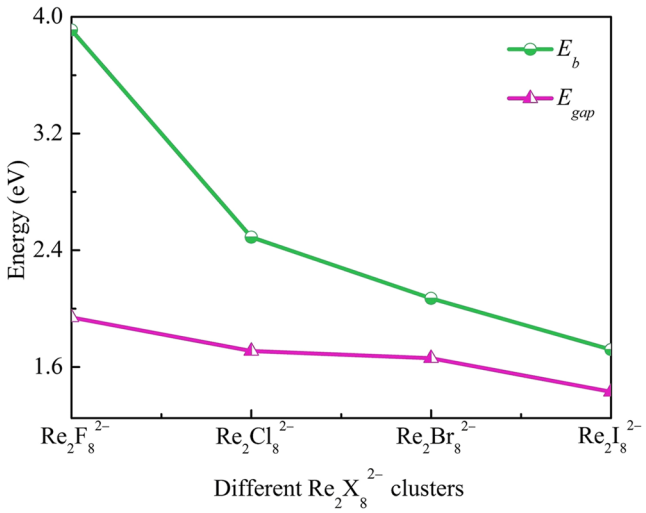

Figure 3. The average binding energies per atom E_b and HOMO−LUMO energy gaps of $Re_2X_8^{2-}$ (X = F, Cl, Br, I).

simulated PES of $Re_2Cl_8^{2-}$, the ADE, namely the second electron binding energy, is 0.98 eV, which is consistent with the experimental datum of 1.00 eV. The first peak is located at 1.19 eV, in reasonable agreement with the first peak location of the experimental spectrum of $Re_2Cl_8^{2-}$ centered at 1.16 eV. The following three peaks are relatively intense, located at 2.21, 2.80, and 3.24 eV, respectively. In the simulated PES of $Re_2Br_8^{2-}$, the first peak is quite intense, and emerges at 2.09 eV. In addition, there is a relatively sharp peak, which is the most intense one, located at 3.95 eV. The simulated spectrum of $Re_2I_8^{2-}$ exhibits three obviously intense peaks and the first relatively weak peak emerges at 1.21 eV. The agreement of the ADE and VDE values of the simulated and experimental PES for $Re_2Cl_8^{2-}$ supports the validity of our computational approach. We hope that the simulated PES of dirhenium halides can provide a helpful reference for the spectroscopic studies of $Re_2X_8^{2-}$ (X = F, Br, I) dianions.

Relative Stabilities. To explore the relative stabilities of the ground state structures of the dirhenium halide system, we have calculated the average binding energies (E_b). For $Re_2X_8^{2-}$ (X = F, Cl, Br, I) clusters, the E_b can be defined as follow:

$$E_b = [2E(\mathrm{Re}) + 6E(\mathrm{X}) + 2E(\mathrm{X}^-) - E(\mathrm{Re_2X_8}^{2-})]/10 \quad (1)$$

Where $E(Re_2X_8^{2-})$, $E(Re)$, $E(X)$, and $E(X^-)$ represent the energy of $Re_2X_8^{2-}$ clusters, neutral Re atom, neutral X atom, and anionic X^-, respectively. The average binding energies of $Re_2X_8^{2-}$ (X = F, Cl, Br, I) clusters are displayed in Fig. 3. From Fig. 3 we can find that $Re_2F_8^{2-}$ is relatively stable due to its large average binding energy value. Besides, the E_b values of $Re_2X_8^{2-}$ decrease monotonically from $Re_2F_8^{2-}$ to $Re_2I_8^{2-}$, indicating that the relative stabilities of $Re_2X_8^{2-}$ (X = F, Cl, Br, I) decrease with increasing size of the halogen atom.

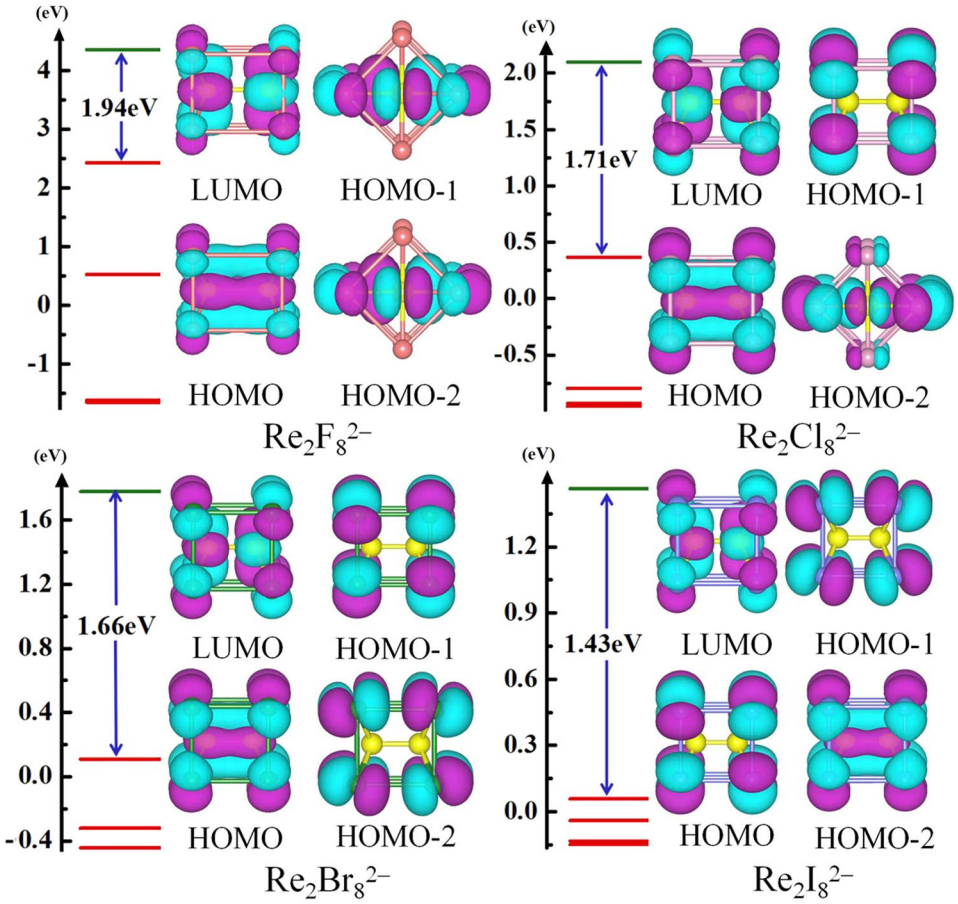

Figure 4. Molecular orbital maps and energy levels of $Re_2X_8^{2-}$ (X = F, Cl, Br, I). The HOMO−LUMO energy gap is indicated (in blue).

Another important parameter related to the relative stabilities of the $Re_2X_8^{2-}$ clusters is the HOMO−LUMO energy gap (E_{gap}), which represents the ability of an electron to jump from the highest occupied molecular orbital (HOMO) to the lowest unoccupied molecular orbital (LUMO). A large value of E_{gap} implies the corresponding molecular structure is chemically inert. The evolution of the HOMO−LUMO energy gap for the ground-state $Re_2X_8^{2-}$ clusters is shown in Fig. 3. It is clearly seen that the E_{gap} decrease monotonically, that is to say, the clusters are relatively less reactive as the halogen atom size increases, in agreement with the obtained results for the average binding energies. However, in contrast to the average binding energy rapid decrease from $Re_2F_8^{2-}$ to $Re_2I_8^{2-}$, the HOMO−LUMO energy gap decreases less steeply.

Charge Transfer. Electronegativity[35–39] is an important chemical property to describe the ability of an atom to attract electrons. A large electronegativity value is interpreted as a strong ability to attract electrons. In order to investigate the charge transfer between Re atoms and halogen atoms for ground-state $Re_2X_8^{2-}$ clusters and compare to the electronegativity, we utilize natural population analysis (NPA) to obtain the charge on each atom. The results are summarized in Table 1. From Table 1 we can see that the negative charge on halogens gradually decreases from $Re_2F_8^{2-}$ to $Re_2I_8^{2-}$. This phenomenon agrees with the decreasing values of Pauling electronegativity, which are 3.98, 3.16, 2.96 and 2.66[40] for F, Cl, Br and I, respectively. Meanwhile, the charge on Re changes from positive to negative and the negative charge on Re is increasing with the halogen atom size increasing. All this indicates that it becomes more competitive for Re to attract electrons as the electronegativity values of halogens decrease. Although the electronegativity value of Re (1.93 on the Pauling scale)[36] is lower than that of all halogen atoms, the negative charge on Re atoms is more than that of Br and I for $Re_2Br_8^{2-}$ and $Re_2I_8^{2-}$, clearly not in accord with the electronegativity. This is perhaps related to the weak ability of Br and I halogen atoms to attract electrons caused by their large atomic radii and the strong intramolecular Coulomb repulsion observed in multiply charged anions[34]. In summary, the two excess negative charges shift from peripheral halogens to Re atoms in the case of heavier halogen atoms.

Chemical Bonding Analysis. In order to explore the nature of the chemical bonding in $Re_2X_8^{2-}$, we have carried out a detailed analysis on the HOMO−LUMO molecular orbitals (MOs). Figure 4 shows the molecular orbital diagrams of $Re_2X_8^{2-}$ clusters together with their orbital energy levels, which feature their HOMO−LUMO energy gaps. Herein we take the Re–Re bond as z axis and the Re–Cl bond as $\pm x$ and $\pm y$ axes to analyze the

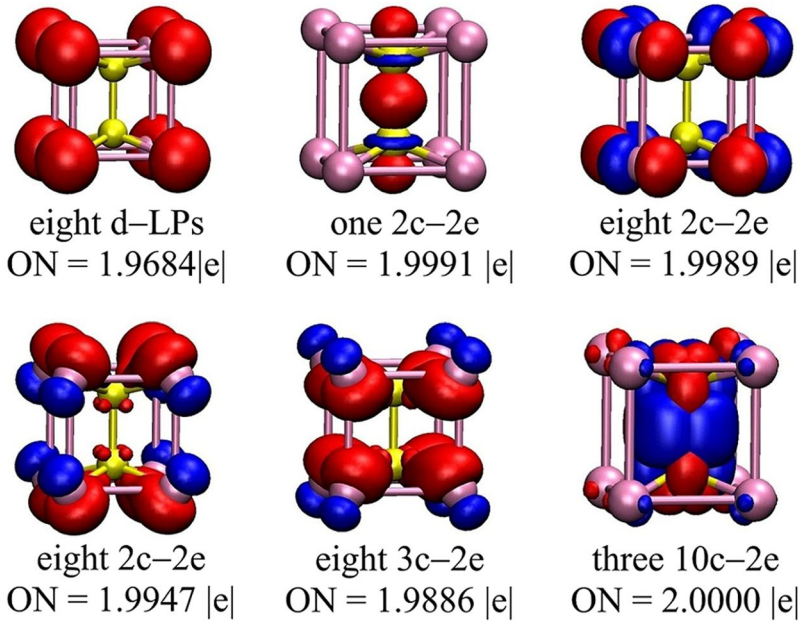

Figure 5. The results of AdNDP analysis for $Re_2Cl_8^{2-}$. ON represents the occupation number.

chemical bonding. As shown in Fig. 4, the HOMO of $Re_2F_8^{2-}$ displays a large overlap between the $5d_{xy}$ orbitals of the two Re atoms, and the overlap forms a δ bond. The HOMO−1 and HOMO−2 are doubly degenerate, which feature π bonds formed by the overlap of the $5d_{yz}$ orbitals. From the HOMO of $Re_2Cl_8^{2-}$, it can be seen that the $5d_{xy}$ orbitals of the Re atoms overlap and this leads to the formation of the δ bond. In $Re_2Cl_8^{2-}$, the HOMO-2 and HOMO−3 are doubly degenerate, leading to π bonds formation by the overlap of the $5d_{yz}$ orbitals. In the HOMO of $Re_2Br_8^{2-}$, the $5d_{xy}$ orbitals of Re atoms have an overlap, leading to the formation of the δ bond. As for $Re_2I_8^{2-}$, there is no bonding between Re and Re in HOMO, while the HOMO-2 reveals an overlap between the $5d_{xy}$ orbitals of the Re atoms, forming a δ bond. Both the HOMO of $Re_2X_8^{2-}$ (X=F, Cl, Br) and the HOMO−2 of $Re_2I_8^{2-}$ are δ bonds. Compared to σ and π bonds[10,13,21], the δ bond is weak and contributes relatively a little to the total strength of the Re–Re bond. Nevertheless, it plays a vital role in geometric structure. The δ bond strength achieves its maximum only when the conformation is eclipsed. Its strength reduces as the conformation becomes staggered[19]. Thus, we can deduce that the δ bond is the pivotal factor for the ground-state $Re_2X_8^{2-}$ (X = F, Cl, Br, I) clusters to maintain D_{4h} symmetric cube-like structures.

To further understand the bonding mechanism in $Re_2X_8^{2-}$, we select $Re_2Cl_8^{2-}$ as a representative example in order to perform a chemical bonding analysis using the adaptive natural density partitioning (AdNDP) method, which is particularly suitable to decipher the nature of the chemical bond. The AdNDP results displayed in Fig. 5 reveals 25 localized bonds and 11 delocalized bonds with occupation numbers (ONs) ranging from 1.9684 to 2.0000 |e|, very close or nearly equal to the ideal values (2.000 |e|). There are eight 1c–2e lone pairs (3 s) with the ON of 1.9684 |e|. The seventeen 2c–2e bonds can be divided into three sets, which contain one Re–Re bond (ON = 1.9991 |e|), eight Cl–Cl bonds (ON = 1.9989 |e|), and eight Re–Cl bonds (ON = 1.9947 |e|), respectively. The Re–Re bond is formed by the overlap of 5d orbital between the two Re atoms. For the Cl–Cl bonds, the 3p orbital in the peripheral Cl atoms results in the formation of the 2c–2e bonds. The interaction between Re and Cl is mainly dominated by the 5d orbital of Re atom and the 3p orbital of the Cl atom. The eight 3c–2e bonds with ON = 1.9886 |e| are formed by the 5d orbitals of two Re atoms and the 3p orbital of one Cl atom. There are three 10c−2e bonds with the ONs of 2.0000 |e| between the two Re atoms and the Cl_8 framework, which strengthen the interactions between the inside Re atoms and the peripheral Cl atoms. In addition, the high occupation number among the localized and delocalized bonds may point to its stability. Overall, the enhanced stability of $Re_2Cl_8^{2-}$ is mainly caused by the chemical bonding of 5d orbital of Re atoms and 3p orbital of Cl atoms.

Conclusions

We have performed a comprehensive research on the structural and electronic properties of dirhenium halide clusters via unbiased CALYPSO structure searches combined with DFT optimizations. The results clearly reveal that the ground states of $Re_2X_8^{2-}$ (X = F, Cl, Br, I) all possess cube-like geometry with D_{4h} symmetry. This finding has been further tested by performing calculations at the BP86 level. The simulated PES of $Re_2Cl_8^{2-}$ shows reasonable agreement with the experimental spectrum, which further confirms the validity of our computational approach. According to the average binding energy and HOMO−LUMO energy gap, $Re_2X_8^{2-}$ clusters are progressively less stable as halogen atoms become heavier. The chemical bonding analysis indicates that the δ bond is the pivotal factor for the ground-state $Re_2X_8^{2-}$ (X = F, Cl, Br, I) clusters to retain D_{4h} symmetric cube-like structures, and the enhanced stability of $Re_2Cl_8^{2-}$ is mainly due to the chemical bonding of 5d orbital of Re atoms

and 3p orbital of Cl atoms. We expect our findings provide stimulations and guidance to researchers for further experimental or theoretical investigations on binuclear transition metal halide clusters.

Computational Method

The low-lying isomers of $Re_2X_8^{2-}$ (X = F, Cl, Br, I) clusters are determined via the CALYPSO method which is based on the particle swarm optimization (PSO) algorithm. This theoretical method has been described in sufficient detail previously[41–43]. In brief, it can explore the global minima of the potential energy surfaces of predicted system only based on the chemical compositions at given external conditions. It has achieved great success in predicting the ground-state structures of various systems[44–49]. Herein, initial structures for $Re_2X_8^{2-}$ clusters are achieved by the CALYPSO method. Each generation contains 50 structures and 60% of those are generated by PSO, while the other structures are generated randomly. We have followed 30 generations for each cluster to achieve convergence to the global minima on the potential energy surfaces. The candidates within 4 eV of the lowest-energy structure are further optimized using the B3LYP[50,51] exchange-correlation functional. The 6-311 + G(d) basis set for F and the LANL2DZ[52,53] basis with effective core potentials for Cl, Br, I and transition-metal Re are employed throughout all calculations. All these calculations are carried out using the Gaussian 09 software package[54]. The choice of the B3LYP functional and The LANL2DZ basis leans heavily on experience acquired from the previous investigations[11,13,55]. Different spin multiplicities are taken into consideration in the geometric optimization process (up to quintet for all clusters). The harmonic vibrational frequencies are calculated in order to ensure that the optimized structures are true minima without any imaginary frequencies. We also perform the natural bond orbital (NBO)[56] and adaptive natural density partitioning (AdNDP)[57] to get further insight into the chemical bonding mechanism.

In order to identify the reliability of our calculations, we have optimized the structures of dirhenium halide clusters with the non-hybrid BP86 functional and the same basis set as above. It is readily seen that the optimized results of $Re_2X_8^{2-}$ clusters obtained by BP86 method are in accordance with our B3LYP results. In addition, compared with the Re–Re bond length of $Re_2X_8^{2-}$ dianions in previous study[2] (Table S4), we can see the results calculated by the B3LYP level agree better than those from the BP86 functional. Thus we conclude that the results obtained at B3LYP level are reliable. To further confirm the reliability of our computational method, we simulate the photoelectron spectra (PES) of all lowest-energy dirhenium halide clusters and compare to the available experimental PES[21]. The first VDE is obtained based on the energy difference between the singly charged anion and dianion at the ground-state geometry of the dianion. The excited-state energies of the singly charged anion are calculated via the time-dependent density functional theory (TD-DFT) method[58]. The reasonable agreement between the simulated and the experimental PES of $Re_2Cl_8^{2-}$ strongly supports our choice of B3LYP functional.

References

1. Cotton, F. A. *et al*. Mononuclear and polynuclear chemistry of rhenium(III): Its pronounced homophilicity. *Science* **145**, 1305–1307 (1964).
2. Cotton, F. A., Murillo, C. A. & Walton, R. A. *Multiple Bonds Between Metal Atoms*. **8**, 271−280. (Springer Science and Business Media, Inc., New York, 2005).
3. Cotton, F. A. Highlights from recent work on metal−metal bonds. *Inorg. Chem.* **37**, 5710–5720 (1998).
4. Cotton, F. A., Curtis, N. F., Johnson, B. F. G. & Robinson, W. R. Compounds containing dirhenium(III) octahalide anions. *Inorg. Chem.* **4**, 326–330 (1965).
5. Barder, T. J. & Walton, R. A. Reductive coupling of perrhenate to form the octachlorodirhenate(III) anion: A new, convenient, and high-yield synthetic procedure. *Inorg. Chem.* **21**, 2510–2511 (1982).
6. Shtemenko, A. V., Kozhura, O. V., Pasenko, A. A. & Domasevitch, K. V. New octachlorodirhenate(III) salts: Solid state manifestation for a certain conformational flexibility of the $[Re_2Cl_8]^{2-}$ ion. *Polyhedron* **22**, 1547–1552 (2003).
7. Cotton, F. A. & Harris, C. B. The crystal and molecular structure of dipotassium octachlorodirhenate(III) dihydrate, $K_2[Re_2Cl_8]\cdot 2H_2O$. *Inorg. Chem.* **4**, 330–333 (1965).
8. Cotton, F. A., Frenz, B. A., Stults, B. R. & Webb, T. R. Investigations of quadruple bonds by polarized crystal spectra. I. The interpretation of the spectrum of tetra(*n*-butylammonium) octachlorodirhenate. The disordered crystal structure. *J. Am. Chem. Soc.* **98**, 2768–2773 (1976).
9. Cotton, F. A. Metal–metal bonding in $[Re_2X_8]^{2-}$ ions and other metal atom clusters. *Inorg. Chem.* **4**, 334–336 (1965).
10. Cotton, F. A. & Harris, C. B. Molecular orbital calculations for complexes of heavier transition elements. III. The metal–metal bonding and electronic structure of $Re_2Cl_8^{2-}$. *Inorg. Chem.* **6**, 924–929 (1967).
11. Ponec, R. & Yuzhakov, G. Metal–metal bonding in $Re_2Cl_8^{(2-)}$ from the analysis of domain averaged fermi holes. *Theor. Chem. Acc.* **118**, 791–797 (2007).
12. Krapp, A., Lein, M. & Frenking, G. The strength of the σ-, π- and δ-bonds in $Re_2Cl_8^{2-}$. *Theor. Chem. Acc.* **120**, 313–320 (2008).
13. Ponec, R., Bučinský, L. & Gatti, C. Relativistic effects on metal–metal bonding: Comparison of the performance of ECP and scalar DKH description on the picture of metal–metal bonding in $Re_2Cl_8^{2-}$. *J. Chem. Theory Comput.* **6**, 3113–3121 (2010).
14. Hay, P. J. Ab initio studies of the metal–metal bond in octachlorodirhenate(2−). *J. Am. Chem. Soc.* **100**, 2897–2898 (1978).
15. Cowman, C. D. & Gray, H. B. Low-temperature polarized spectral study of the lowest electronic absorption band in $Re_2Cl_8^{2-}$ and related binuclear complexes. *J. Am. Chem. Soc.* **95**, 8177–8178 (1973).
16. Mortola, A. P., Moskowitz, J. W., Rösch, N., Cowman, C. D. & Gray, H. B. Electronic structure of $Re_2Cl_8^{2-}$. *Chem. Phys. Lett.* **32**, 283–286 (1975).
17. Trogler, W. C., Cowman, C. D., Gray, H. B. & Cotton, F. A. Further studies of the electronic spectra of octachlorodirhenate(2−) and octabromodirhenate(2−). Assignment of the weak bands in the 600−350-nm region. Estimation of the dissociation energies of metal–metal quadruple bonds. *J. Am. Chem. Soc.* **99**, 2993–2996 (1977).
18. Trogler, W. C. & Gray, H. B. Electronic spectra and photochemistry of complexes containing quadruple metal–metal bonds. *Acc. Chem. Res.* **11**, 232–239 (1978).
19. Cotton, F. A. Spectroscopic and quantum theoretical studies of species with metal–to–metal bonds. *J. Mol. Struct.* **59**, 97–108 (1980).
20. Hay, P. J. Electronic states of the quadruply bonded $Re_2Cl_8^{2-}$ species: An ab initio theoretical study. *J. Am. Chem. Soc.* **104**, 7007–7017 (1982).
21. Wang, X. B. & Wang, L. S. Probing the electronic structure and metal–metal bond of $Re_2Cl_8^{2-}$ in the gas phase. *J. Am. Chem. Soc.* **122**, 2096–2100 (2000).
22. Gagliardi, L. & Roos, B. O. The electronic spectrum of $Re_2Cl_8^{2-}$: A theoretical study. *Inorg. Chem.* **42**, 1599–1603 (2003).

23. Cotton, F. A., Deboer, B. G. & Jeremic, M. Some reactions of the octahalodirhenate (III) ions. VIII. Definitive structural characterization of the octabromodirhenate (III) ion. *Inorg. Chem.* **9**, 2143–2146 (1970).
24. Huang, H. W. & Martin, D. S. Single-crystal polarized spectra for the $\delta \rightarrow \delta^*$ band of tetrabutylammonium octachlorodirhenate(III) and tetrabutylammonium octabromodirhenate(III). Crystal structure of the octabromo salt. *Inorg. Chem.* **24**, 96–101 (1985).
25. Peters, G. & Preetz, W. Synthesis and properties of the octafluorodirhenate(III) anion, $[Re_2F_8]^{2-}$. *Z. Naturforsch.* **34**, 1767−1768 (1979).
26. Conradson, S. D., Sattelberger, A. P. & Woodruff, W. H. X-ray absorption study of octafluorodirhenate(III): EXAFS structures and resonance Raman spectroscopy of octahalodirhenates. *J. Am. Chem. Soc.* **110**, 1309–1311 (1988).
27. Henkel, G., Peters, G., Preetz, W. & Skowronek, J. Crystal structure and vibration spectra of $[(n\text{-}C_4H_9)_4N]_2[Re_2F_8]\cdot 2(C_2H_5)_2O$. *Z. Naturforsch.* **45**, 469–475 (1990).
28. Balasekaran, S. M. *et al*. Octafluorodirhenate(III) revisited: Solid-state preparation, characterization, and multiconfigurational quantum chemical calculations. *Inorg. Chem.* **55**, 5417–5421 (2016).
29. Glicksman, H. D. & Walton, R. A. Studies on metal carboxylates. 14. Reactions of molybdenum(II) and rhenium(III) carboxylates with the gaseous hydrogen halides in alcoholic media. Synthesis, characterization, and reactivity of the new haloanions of molybdenum and rhenium, $Mo_2Br_6^-$, $Mo_4I_{11}^{2-}$, and $Re_2I_8^{2-}$. *Inorg. Chem.* **17**, 3197–3202 (1978).
30. Preetz, W. & Rudzik, L. Synthesis and properties of tetrabutylammonium octaiododirhenate(III), $[(n\text{-}C_4H_9)_4N]_2[Re_2I_8]$. *Angew. Chem. Int. Ed. Engl.* **18**, 150–151 (1979).
31. Preetz, W., Peters, G. & Rudzik, L. Resonance Raman spectrum of tetrabutylammonium octaiododirhenate(III), $[(n\text{-}C_4H_9)_4N]_2[Re_2I_8]$. *Z. Naturforsch.* **34**, 1240–1242 (1979).
32. Cotton, F. A., Daniels, L. M. & Vidyasagar, K. The crystal structure of $[(n\text{-}C_4H_9)_4N]_2Re_2I_8$: Three-fold disorder of the effectively cubic anion. *Polyhedron* **7**, 1667−1672 (1988).
33. Wang, X. B., Yang, X. & Wang, L. S. Probing solution-phase species and chemistry in the gas phase. *Int. Rev. Phys. Chem.* **21**, 473–498 (2002).
34. Dreuw, A. & Cederbaum, L. S. Multiply charged anions in the gas phase. *Chem. Rev.* **102**, 181–200 (2002).
35. Pauling, L. The nature of the chemical bond. IV. The energy of single bonds and the relative electronegativity of atoms. *J. Am. Chem. Soc.* **54**, 3570–3582 (1932).
36. Gordy, W. & Thomas, W. J. O. Electronegativities of the elements. *J. Chem. Phys.* **24**, 439–444 (1956).
37. Allred, A. L. & Rochow, E. G. A scale of electronegativity based on electrostatic force. *J. Inorg. Nucl. Chem.* **5**, 264–268 (1958).
38. Allred, A. L. Electronegativity values from thermochemical data. *J. Inorg. Nucl. Chem.* **17**, 215–221 (1961).
39. Parr, R. G., Donnelly, R. A., Levy, M. & Palke, W. E. Electronegativity: The density functional viewpoint. *J. Chem. Phys.* **68**, 3801–3807 (1978).
40. Murphy, L. R., Meek, T. L., Allred, A. L. & Allen, L. C. Evaluation and test of Pauling's electronegativity scale. *J. Phys. Chem. A* **104**, 5867–5871 (2000).
41. Wang, Y. C., Lv, J., Zhu, L. & Ma, Y. M. Crystal structure prediction via particle-swarm optimization. *Phys. Rev. B* **82**, 094116 (2010).
42. Wang, Y. C., Lv, J., Zhu, L. & Ma, Y. M. CALYPSO: A method for crystal structure prediction. *Comput. Phys. Commun.* **183**, 2063−2070 (2012).
43. Lv, J., Wang, Y. C., Zhu, L. & Ma, Y. M. Particle-swarm structure prediction on clusters. *J. Chem. Phys.* **137**, 084104 (2012).
44. Zhu, L. *et al*. Substitutional alloy of Bi and Te at high pressure. *Phys. Rev. Lett.* **106**, 145501 (2011).
45. Zhu, L., Liu, H. Y., Pickard, C. J., Zou, G. T. & Ma, Y. M. Reactions of xenon with iron and nickel are predicted in the earth's inner Core. *Nat. Chem.* **6**, 644–648 (2014).
46. Lv, J., Wang, Y. C., Zhu, L. & Ma, Y. M. Predicted novel high-pressure phases of lithium. *Phys. Rev. Lett.* **106**, 015503 (2011).
47. Xing, X. D. *et al*. Insights into the geometries, electronic and magnetic properties of neutral and charged palladium clusters. *Sci. Rep-uk.* **6**, 19656 (2016).
48. Jin, Y. Y. *et al*. Probing the structural evolution of ruthenium doped germanium clusters: Photoelectron spectroscopy and density functional theory calculations. *Sci. Rep-uk.* **6**, 30116 (2016).
49. Ding, L. P., Shao, P., Lu, C., Zhang, F. H. & Wang, L. Y. Iron-based magnetic superhalogens with pseudohalogens as ligands: An unbiased structure search. *Sci. Rep-uk.* **7**, 45149 (2017).
50. Becke, A. D. Density functional thermochemistry. III. The role of exact exchange. *J. Chem. Phys.* **98**, 5648–5652 (1993).
51. Lee, C., Yang, W. & Parr, R. G. Development of the Colle-Salvetti correlation-energy formula into a functional of the electron density. *Phys. Rev. B* **37**, 785–789 (1988).
52. Wadt, W. R. & Hay, P. J. Ab initio effective core potentials for molecular calculations. Potentials for main group elements Na to Bi. *J. Chem. Phys.* **82**, 284–298 (1985).
53. Hay, P. J. & Wadt, W. R. Ab initio effective core potentials for molecular calculations. Potentials for K to Au including the outermost core orbitals. *J. Chem. Phys.* **82**, 299–310 (1985).
54. Frisch, M. J. *et al.* Gaussian 09 (Revision C.0). Gaussian, Inc., Wallingford, CT, 2009. URL http://www.gaussian.com.
55. Taylor, C. J., Wu, B., Nix, M. G. D. & Dessent, C. E. H. Probing the gas-phase stability of the $Re_2X_8^{2-}$ (X = Cl, Br) and $Re_2X_nY_{8-n}^{2-}$ (X = Cl, Y = Br, n = 1−3) metal–metal bond complexes. *Chem. Phys. Lett.* **479**, 184–188 (2009).
56. Read, A. E., Curtiss, L. A. & Weinhold, F. Intermolecular interactions from a natural bond orbital, donor–acceptor viewpoint. *Chem. Rev.* **88**, 899–926 (1988).
57. Zubarev, D. Y. & Boldyrev, A. I. Developing paradigms of chemical bonding: Adaptive natural density partitioning. *Phys. Chem. Chem. Phys.* **10**, 5207–5217 (2008).
58. Casida, M. E., Jamorski, C., Casida, K. C. & Salahub, D. R. Molecular excitation energies to high-lying bound states from time-dependent density-functional response theory: Characterization and correction of the time-dependent local density approximation ionization threshold. *J. Chem. Phys.* **108**, 4439–4449 (1998).

Acknowledgements

This work was supported by the National Natural Science Foundation of China (Grants 11574220, 11304167, and 21671114), the 973 Program of China (Grant 2014CB660804), the Special Program for Applied Research on Super Computation of the NSFC–Guangdong Joint Fund (the second phase; Grant U1501501), and the Program for Science & Technology Innovation Talents in Universities of Henan Province (Grant 15HASTIT020).

Author Contributions

C.L. and X.Y.K. conceived the idea. L.H.Z., X.X.X. and C.L. performed the calculations. L.H.Z., X.X.X., W.G.S. B.L.C. and G.M. wrote the manuscript.

Additional Information

Supplementary information accompanies this paper at https://doi.org/10.1038/s41598-018-25027-1.

Competing Interests: The authors declare no competing interests.